Title: A deeper insight into (Lu,Y)AG : Pr scintillator crystals

Author: W. Drozdowski, A.J. Wojtowicz, K. Brylew, W. Łachmański, Ewa Talik, Magdalena Szubka, Joachim Kusz, Adam Guzik, Katarzyna Balin i in.

Citation style: Drozdowski W., Wojtowicz A.J., Brylew K., Łachmański W., Talik Ewa, Szubka Magdalena, Kusz Joachim, Guzik Adam, Balin Katarzyna i in. (2017). A deeper insight into (Lu,Y)AG : Pr scintillator crystals. "IOP Conference Series: Materials Science and Engineering" (Vol. 169, iss. 1 (2017), Article number 012010), doi 10.1088/1757-899X/169/1/012010

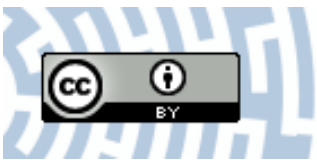

A deeper insight into (Lu,Y)AG:Pr scintillator crystals

W. Drozdowski[1], A.J. Wojtowicz[1], K. Brylew[1], W. Łachmański[1], E. Talik[2], M. Szubka[2], J. Kusz[2], A. Guzik[2], K. Balin[3], J. Kisielewski[4], M. Świrkowicz[4] and A. Pajączkowska[4]

[1]Institute of Physics, Faculty of Physics, Astronomy and Informatics, Nicolaus Copernicus University, Grudziadzka 5, 87-100 Torun, Poland
[2]Institute of Physics, University of Silesia, Uniwersytecka 4, 40-007 Katowice, Poland
[3]Silesian Center for Education and Interdisciplinary Research, University of Silesia, 75 Pulku Piechoty 1A, 41-500 Chorzow, Poland
[4]Institute of Electronic Materials Technology, Wolczynska 133, 01-919 Warsaw, Poland

E-mail: wind@fizyka.umk.pl

Abstract. Interior of Czochralski-grown (Lu,Y)AG:Pr crystals has been examined by means of several techniques, such as X-Ray Photoelectron Spectroscopy, X-Ray Diffraction, Time-of-Flight Secondary Ion Mass Spectrometry, and magnetic susceptibility measurements. Additionally, their luminescence has been monitored at various combinations of a double-beam (X-ray/IR) excitation.

1. Introduction

Mixed (Lu,Y)AG:Pr crystals have already been recognized as promising fast and efficient scintillator materials. Compared to their prototype LuAG:Pr they offer higher light outputs and increased contributions of the prompt component to their scintillation time profiles at an expense of a somewhat lower density [1,2]. In this Communication we provide additional data on the internal structure of Czochralski-grown (Lu,Y)AG:Pr crystals, as well as on some trap-related aspects of their scintillation mechanism. Our research comprises X-Ray Photoelectron Spectroscopy (XPS), X-Ray Diffraction (XRD), Time-of-Flight Secondary Ion Mass Spectrometry (ToF-SIMS), measurements of magnetic susceptibility as a function of temperature, and advanced experiments with a coupled X-ray and infrared (IR) excitation.

2. Materials and experiment

The crystals of pure and Pr-activated $(Lu_xY_{1-x})_3Al_5O_{12}$ (x = 0.00, 0.25, 0.50, 0.75, 1.00) have been grown at ITME, Warsaw, by the Czochralski method as characterized in [1,2].

XPS spectra have been taken with a PHI 5700/660 Physical Electronics Photoelectron Spectrometer under monochromated Al K_α X-rays (14.86 keV). XRD has been investigated with a four-circle Kuma Diffraction KM-4 diffractometer under graphite-monochromated Mo K_α X-rays (17.48 keV). ToF-SIMS studies have been carried out with a IONTOF TOF.SIMS 5 reflection-type spectrometer equipped with a Bi liquid metal ion gun. The data analysis has been performed with a

SurfaceLab6 software package. Magnetic susceptibility has been measured as a function of temperature between 2 and 400 K using a Quantum Design MPMS-XL-7AC SQUID magnetometer.

Double-beam experiments have been conducted with a setup consisting of an Inel XRG3500 X-ray generator with a Cu-anode tube (45 kV, 10 mA), a Thorlabs IR laser diode (830 nm, 1000 mW, 750 mA), an ARC SpectraPro 500i monochromator, a Hamamatsu R928 photomultiplier, and an APD Cryogenics closed-cycle He cooler with a Lake Shore 330 temperature controller.

3. Results and discussion

3.1. Internal structure studies

3.1.1. XPS. Two representative XPS spectra of $(Lu_xY_{1-x})_3Al_5O_{12}$:Pr ($x$ = 0.75 and 0.25) are shown in Fig. 1. They are clearly dominated by well separated lines related to the crystal constituents, i.e. Lu, Y, Al, and O [3,4]. Besides, there is only a single weak line attributed to none of the above-mentioned elements. It is the C 1*s* line at 285 eV, arising in XPS of most samples due to their surface contamination with trace amounts of C, which is in fact useful for calibration purposes [5]. Based on their XPS spectra, the quality of the (Lu,Y)AG:Pr crystals may be rated very high.

3.1.2. XRD. The lattice parameters (*LP*) of $(Lu_xY_{1-x})_3Al_5O_{12}$:Pr read out from XRD measurements are specified in Table 1 and depicted in Fig. 2 as a function of x. It can easily be noticed that *LP* decreases linearly with x, which correlates with the smaller ionic radius of Lu^{3+} compared to Y^{3+} [6] and satisfies the Vegard's law [7]. We note that the values of both the slope (m = 0.091 Å) and the intercept (LP_0 = 12.01 Å) derived from a straight line fit:

$$LP = -mx + LP_0 \tag{1}$$

are in a full accordance with the data of Kuwano *et al.* [8]. Since the particular *LP* points do not lie perfectly on this line, there must be some discrepancies between the initial (in the melt) and the real Lu-to-Y ratios in the mixed crystals, nevertheless their magnitude is very small.

3.1.3. ToF-SIMS. The performed surface imaging and depth profiling, providing information on the chemical composition of the (Lu,Y)AG:Pr crystals, confirm their high purity. A representative case is illustrated by Fig. 3, containing a depth profile of LuAG:Pr. The spatial distribution of the crystal constituents (Lu, Al, O, Pr) can be regarded as uniform. Although some other elementary (H, Li, C, Na, Mg, Si, K, Ca, Ti, Fe, Cu, Zn) and molecular ions appear in the recorded mass spectra, the amount of such contaminations remains at a standard low level, strongly decreasing with depth.

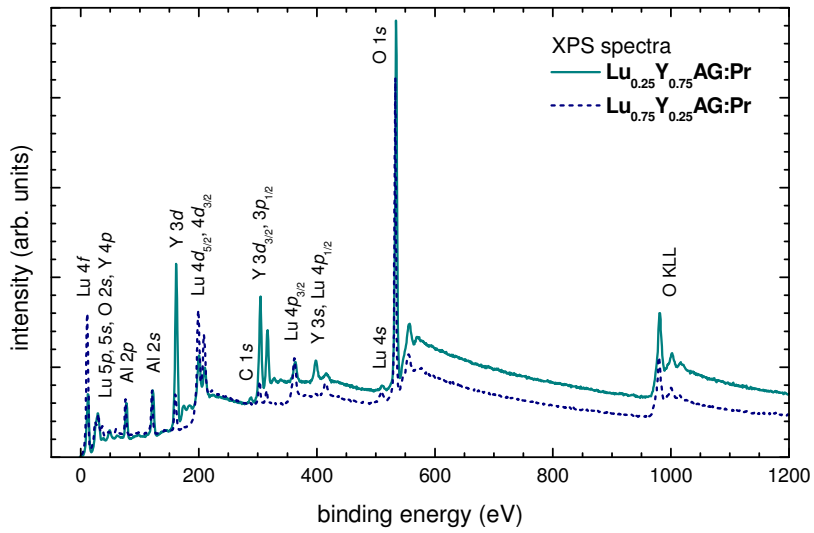

Figure 1. XPS spectra of $Lu_{0.75}Y_{0.25}$AG:Pr and $Lu_{0.25}Y_{0.75}$AG:Pr.

Table 1. Parameters of the studied crystals derived from the XRD and magnetic susceptibility measurements. For a comparison, Pr concentrations determined by the ICP-OES [1] are also listed.

Crystal	*LP* (Å)	χ_0 (10^{-3} emu/mol)	θ (K)	*C* (10^{-3} emu·K/mol)	Pr concentration (at%)	
					magn. susc.	ICP-OES
LuAG	11.917	-0.244	-	-	-	-
LuAG:Pr	11.914	-0.231	-8.3	5.19	0.33	0.12
$Lu_{0.75}Y_{0.25}$AG:Pr	11.940	-0.211	-7.9	5.20	0.33	0.16
$Lu_{0.5}Y_{0.5}$AG:Pr	11.959	-0.230	-11.0	7.71	0.48	0.17
$Lu_{0.25}Y_{0.75}$AG:Pr	11.986	-0.150	-8.0	5.71	0.36	0.23
YAG	12.005	-0.208	-	-	-	-

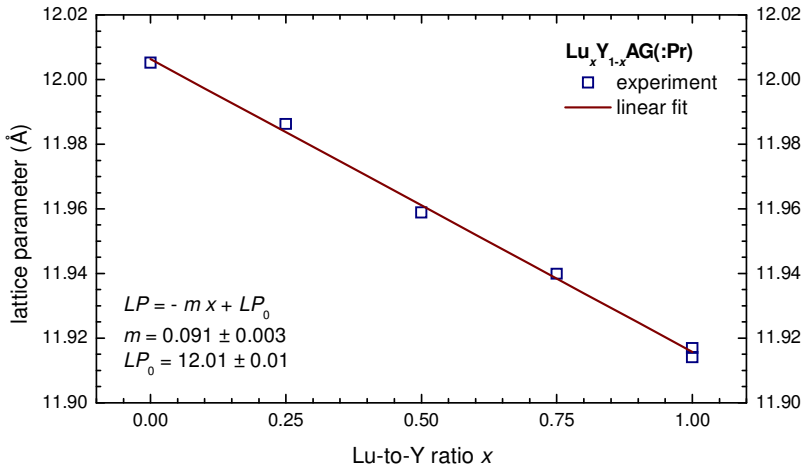

Figure 2. Lattice parameter of $(Lu_xY_{1-x})_3Al_5O_{12}$ as a function of x.

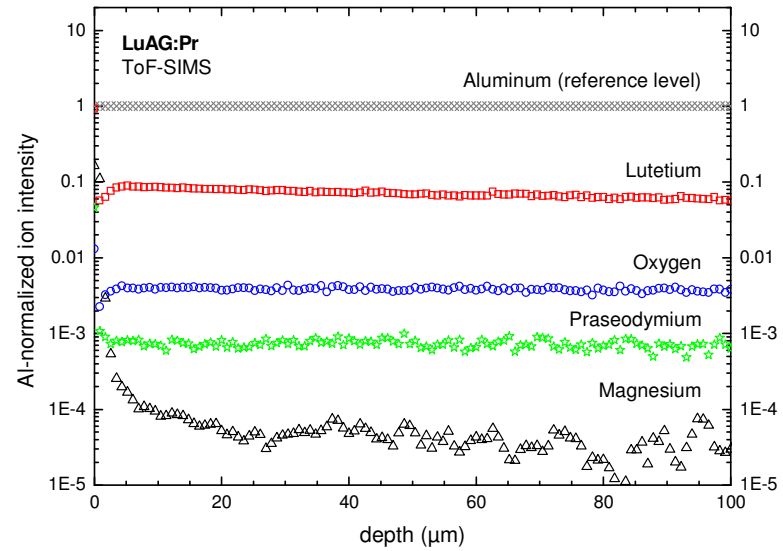

Figure 3. A ToF-SIMS depth profile of LuAG:Pr. Intensities corresponding to the crystal constituents (Lu, O, Pr) and an exemplary contamination (Mg) are normalized to the level of Al.

3.1.4. Magnetic susceptibility. To verify the Pr content determined before by the ICP-OES technique [1], the magnetic susceptibilities χ of the (Lu,Y)AG:Pr crystals have been measured as a function of temperature T (Fig. 4) and thereafter fitted to the known Curie–Weiss law:

$$\chi = \frac{C}{T-\theta} + \chi_0 \qquad (2)$$

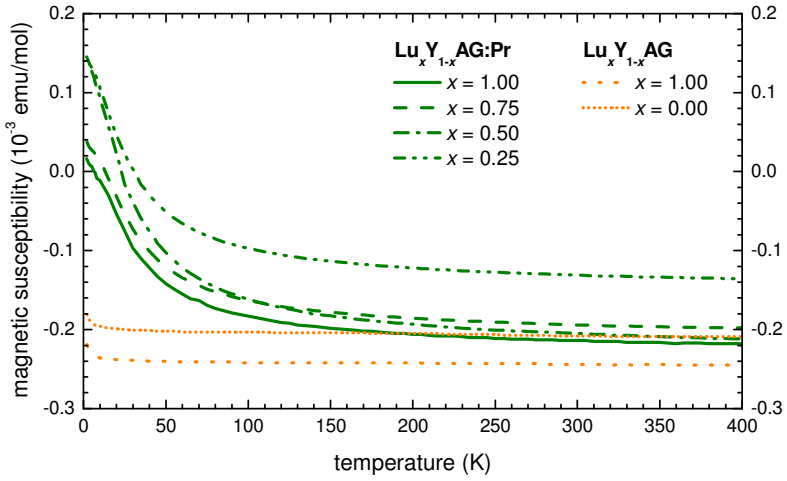

Figure 4. Magnetic susceptibility of (Lu,Y)AG:Pr and (Lu,Y)AG as a function of temperature.

between 50 and 400 K, where C is the Curie constant, θ - the Curie–Weiss temperature, and χ_0 - the temperature-independent diamagnetic susceptibility. The fitting parameters, together with the estimated Pr concentrations using the approach of Talik *et al.* [5], are listed in Table 1. Surprisingly, the obtained concentration values are 2-3 times higher and there is hardly any correlation with the ICP-OES results, which clearly needs a further investigation.

3.2. Double-beam experiments

We have used a novel method proposed by Poolton *et al.* [9] to study the role of traps in the scintillation of (Lu,Y)AG:Pr. During the experiment the luminescence intensity is recorded while the sample is excited by X-rays, X-rays and IR radiation simultaneously, and by IR alone. Both sources are operated independently, but in a sequence to monitor X-ray excited radioluminescence (RL), IR-stimulated luminescence (IR-SL), and RL + IR-SL altogether (Fig. 5). We observe that a longer X-ray irradiation with no IR stimulation leads to a luminescence decay (after switching X-rays off) showing a fast (direct) component and some larger contribution from slow components (afterglow). The time scale of the experiment does not allow any detection of the fast component (radiative lifetime) that is most likely hidden in the direct component. No dominant single exponential decay is present in the IR-SL decays (with or without X-ray excitation). A shorter or no X-ray irradiation is

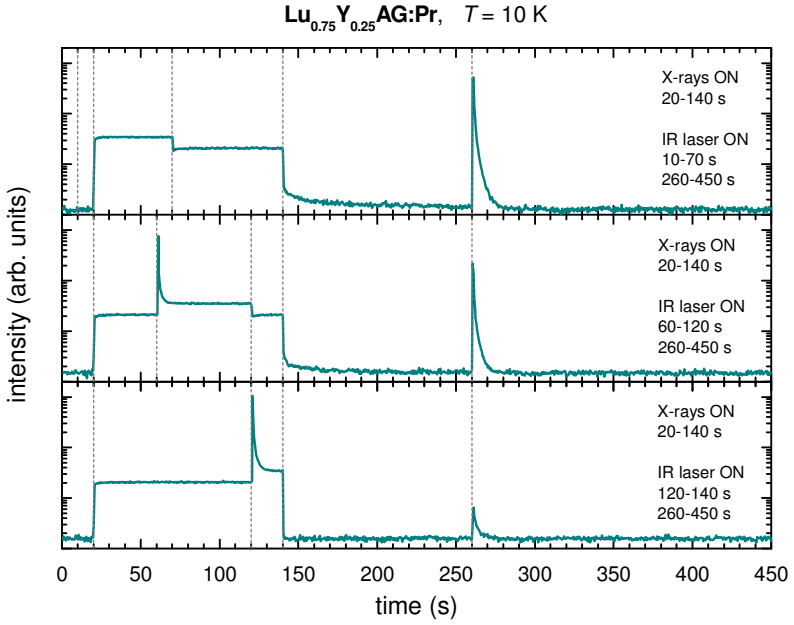

Figure 5. Intensity of the X-ray, IR laser, and X + IR excited luminescence of $Lu_{0.25}Y_{0.75}AG:Pr$ at 10 K vs. time. The emission wavelength is set at 365 nm. The timing and sequence of excitations is indicated in each panel. Note the log scale.

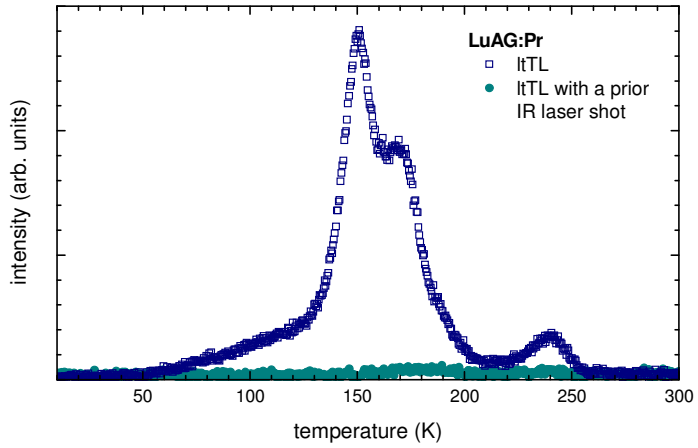

Figure 6. Glow curves of LuAG:Pr, recorded at a heating rate of 0.14 K/s after a standard X-ray irradiation (10 min), with and without a preceding IR laser shot (1 s).

also responsible for a less efficient stimulation by IR, which is consistent with low temperature thermoluminescence (ltTL) measurements: the glow curves in Fig. 6 reveal that all ltTL glow peaks below 250 K are strongly reduced, pointing to traps that contribute to the IR-SL and are emptied by the 830 nm laser irradiation.

It is well known that recombination kinetics can usually be described by a bimolecular law [10]:

$$N = An^2 = \frac{An_0^2}{(n_0 At + 1)^2} \tag{3}$$

where N stands for the number of photons emitted from unit volume per unit time, n – the number of free electrons per unit volume available for recombination, here equal to the number of Pr^{4+} ions [11], whilst the probability that within the time t a given electron will recombine with one of the n available Pr^{4+} ions is equal to Ant. Plotting then:

$$\frac{1}{\sqrt{I}} = \frac{1}{\sqrt{I_0}}(1 + An_0 t) \tag{4}$$

we obtain a decay represented by a straight line.

To check this idea, in Fig. 7 we replot the middle panel of Fig. 5 using the appropriate scale (1/sqrt(intensity)). It is interesting to note that the IR-SL decay, measured after the IR laser is turned on (at 260 s), can be fitted reasonably well with a straight line labeled (a), thus following closely a bimolecular decay law. This is to be expected assuming that *i)* a prior X-ray irradiation fills the traps

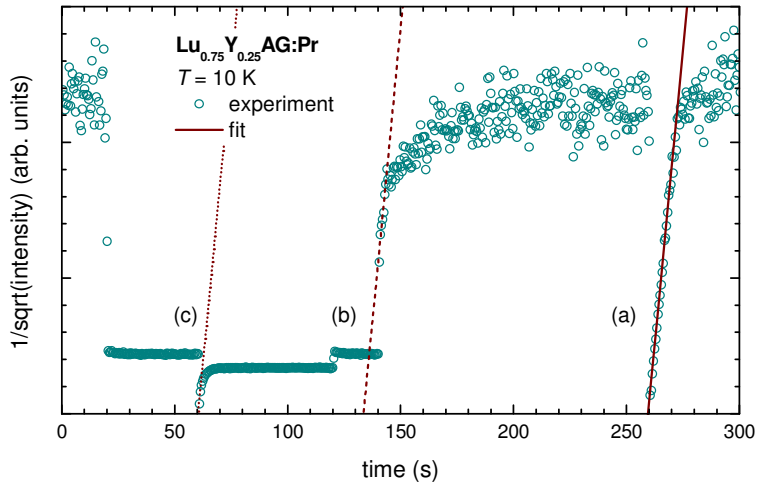

Figure 7. Intensity of the X-ray, IR laser, and X + IR excited luminescence of $Lu_{0.25}Y_{0.75}AG:Pr$ at 10 K vs. time. The emission wavelength is set at 365 nm. The solid (a) straight line is a linear fit to selected experimental points of the IR-SL decay. The dashed (b) and dotted (c) straight lines have the same slope but are shifted to fit different decays. Note the inverse square root scale.

with electrons and generates some population of Pr^{4+} ions, *ii)* electrons are released from traps upon the IR irradiation, *iii)* there is no retrapping of electrons, and *iv)* there is no significant trapping by deeper traps (so that the concentration of Pr^{4+} is not much higher than the number of electrons ready to recombine). The two remaining straight lines in Fig. 7, labeled (b) and (c), have the same slope, but have been shifted to fit the experimental points corresponding to the decays observed when the X-ray and IR excitations are simultaneously turned off (b) or when the IR excitation is turned off but the X-ray excitation remains at a fixed value (c).

It can be noticed in Fig. 7 that unlike for the IR laser stimulation, the decay (b) after the X-ray and IR excitations are turned off follows neither a simple bimolecular law nor a single exponential decay. The experiment, limited in the time resolution, proves nevertheless that there must be an additional component that dominates the shorter times. A simple and obvious explanation is by assuming that in the decay following the X-ray excitation there is a component coming from the direct excitation of Pr^{3+} ions. No such effect is observed in the third decay (c). This decay is dominated by a bimolecular component imposed on the steady-state signal coming from the X-ray excitation.

4. Conclusions

The internal structure research generally confirms a high quality of the grown (Lu,Y)AG:Pr crystals. The only source of concern is the discrepancy between the evaluated Pr concentrations based on two different methods. This issue deserves a further interest.

A bimolecular decay of the X-ray excited sample stimulated by the IR radiation, perceived in the double-beam studies, directly proves that electron transport over the (Lu,Y)AG host is possible. Although the contribution of various processes to scintillation decays may be different than observed in such a kind of a steady-state experiment, the possibility of a bimolecular recombination at activator sites in scintillators should not be overlooked. Finally, since there is no indication of any excitonic transport, the main scintillation mechanism in (Lu,Y)AG:Pr must be a consecutive recombination of first holes and then electrons at Pr sites, which agrees with the previous assumptions [11].

5. References

[1] Drozdowski W, Brylew K, Wojtowicz A J, Kisielewski J, Świrkowicz M, Łukasiewicz T, de Haas J T M and Dorenbos P 2014 *Opt. Mater. Express* **4** 1207-12
[2] Drozdowski W, Brylew K, Witkowski M E, Drewniak A, Masewicz Z, Wojtowicz A J, Kisielewski J and Świrkowicz M 2016 *Opt. Mater.* **59** 107-14
[3] Pawlak D A, Woźniak K, Frukacz Z, Barr T L, Fiorentino D and Seal S 1999 *J. Phys. Chem.* B **103** 1454-61
[4] Kruczek M, Talik E, Sakowska H, Gała M and Świrkowicz M 2005 *Cryst. Res. Technol.* **40** 439-43
[5] Talik E, Zajdel P, Guzik A, Skrzypek D, Lipińska L and Michalska M 2014 *J. Alloys Compd.* **616** 556-68
[6] Shannon R D 1976 *Acta Cryst.* A **32** 751-67
[7] Vegard L 1921 *Z. Phys.* **5** 17-26
[8] Kuwano Y, Suda K, Ishizawa N and Yamada T 2004 *J. Cryst. Growth* **260** 159-65
[9] Poolton N R J, Bos A J J, Wallinga J, de Haas J T M, Dorenbos P, de Vries L, Kars R H, Jones G O and Drozdowski W 2010 *J. Lumin.* **130** 1404-14
[10] Mott N F and Gurney R W 1948 *Electronic processes in ionic crystals* (Oxford: Clarendon Press) p 209
[11] Drozdowski W, Dorenbos P, de Haas J T M, Drozdowska R, Owens A, Kamada K, Tsutsumi K, Usuki Y, Yanagida T and Yoshikawa A 2008 *IEEE Trans. Nucl. Sci.* **55** 2420-4

Acknowledgements

This work has been financed from the funds of the Polish National Science Centre granted on the basis of Decisions no. DEC 2012/05/B/ST5/00324 and DEC 2013/09/N/ST3/01935.